

Residual Stress Formation in Component Related Stress Relief Cracking Tests of a Welded Creep-Resistant Steel

Michael Rhode^{1,2,a,*}, Arne Kromm^{1,b}, Dirk Schroepfer^{1,c},
Joerg Steger^{1,d}, Thomas Kannengiesser^{1,2,e}

¹Bundesanstalt für Materialforschung und -prüfung (BAM), Unter den Eichen 87, 12205 Berlin, Germany

²Otto-von-Guericke University, Universitätsplatz 2, 39106 Magdeburg, Germany

^amichael.rhode@bam.de, ^barne.kromm@bam.de, ^cdirk.schroepfer@bam.de,
^djoergsteger@gmx.de, ^ethomas.kannengiesser@bam.de

Keywords: Welding, Residual Stresses, Creep-Resistant Steel, Post Weld Heat Treatment, Stress Relief Cracking, 13CrMoV9-10

Abstract. Submerged arc welded (SAW) components of creep-resistant low-alloyed Cr-Mo-V steels are used for thick-walled heavy petrochemical reactors (wall-thickness up to 475 mm) as well as employed in construction of modern high-efficient fossil fired power plants. These large components are accompanied by significant restraints during welding fabrication, especially at positions of different thicknesses like welding of nozzles. As a result, residual stresses occur, playing a dominant role concerning so-called stress relief cracking (SRC) typically during post weld heat treatment (PWHT). Besides specific metallurgical factors (like secondary hardening due to re-precipitation), high tensile residual stresses are a considerable influence factor on SRC. For the assessment of SRC susceptibility of certain materials mostly mechanical tests are applied which are isolated from the welding process. Conclusions regarding the influence of mechanical factors are rare so far. The present research follows an approach to reproduce loads, which occur during welding of real thick-walled components scaled to laboratory conditions by using tests designed on different measures. A large-scale slit specimen giving a high restraint in 3 dimensions by high stiffness was compared to a medium-scale multi-pass welding U-profile specimen showing a high degree of restraint in longitudinal direction and a small-scale TIG-re-melted specimen. The small-scale specimens were additionally subjected to mechanical bending to induce loads that are found during fabrication on the real-scale in heavy components. Results show for all three cases comparable high tensile residual stresses up to yield strength with high gradients in the weld metal and the heat affected zone. Those high tensile stresses can be significant for cracking during further PWHT.

Introduction

Safety and economical use of welded components depend to a large extent on reliable welding processing. Submerged arc welding (SAW) is the most important welding technique for creep-resistant steels like the low-alloyed 13CrMoV9-10 for thick-walled components in heavy petrochemical reactors (wall-thickness up to 475 mm) as well as fossil-fired power plants [1, 2]. Those large components are accompanied by significant restraints during welding fabrication, especially at positions of different thicknesses like nozzles. The resulting residual stress state is of immense importance, since highly restrained components tend to stress relief (or relaxation) cracks (SRC) during the final post weld heat treatment (PWHT). SRC phenomenon is determined by the interaction of the design, metallurgical and thermal factors as shown in Fig. 1.



Metallurgical reasons for SRC are differences in strength within the matrix (re-precipitation of carbides at PAGs and the associated secondary hardening) and sufficient tensile stresses which lead to material failure. Those cracks are characterized by intergranular transverse and longitudinal cracks within the weld metal (WM) and the heat affected zone (HAZ). During the PWHT of the welded component, free expansion and shrinkage (relaxation) occur with corresponding local and global stressing of the weld seams. This final manufacturing step is indispensable to set the required material properties for later high-temperature

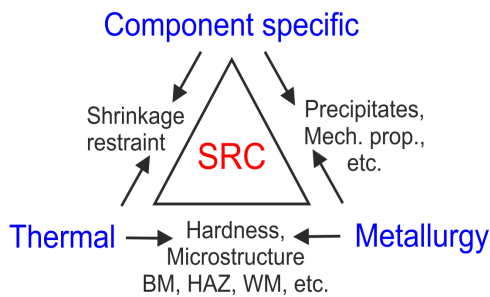


Fig. 1: Influencing factors on SRC [5]

use [3, 4]. Besides specific metallurgical factors, especially high tensile residual stresses are a considerable influence factor on SRC. For assessment of SRC susceptibility, mostly mechanical tests are applied which are isolated from the welding process. Conclusions regarding the influence of mechanical factors are rare so far. For that reason, it is currently not possible to realistically depict the interaction between the mechanical, thermal and metallurgical factors on a laboratory scale. For that purpose, geometry of laboratory specimens was adapted that residual stress state of realistic component-like weld can be simulated [5, 6]. Different stress conditions were set by varying the geometry and welding parameters. The residual stress distributions of a heavy slit sample (Spec A. - 3D-hindered shrinkage due to high restraint, cf. [6]), a medium U-shape notch specimen (Spec. B - high longitudinal shrinkage inhibition) and a small-scale specimen (Spec. C - external loading) were compared. The aim was to investigate if smaller specimens are suitable to represent longitudinal residual stresses as they occur in realistic SAW-manufactured components.

Experimental

Submerged arc welding (SAW) experiments were carried out using the low-alloyed creep-resistant steel 13CrMoV9-10 [7]. The delivered plates had a thickness of 50 mm and three different specimen types Spec. A to C were machined. Specimen dimensions are shown in Fig. 2.

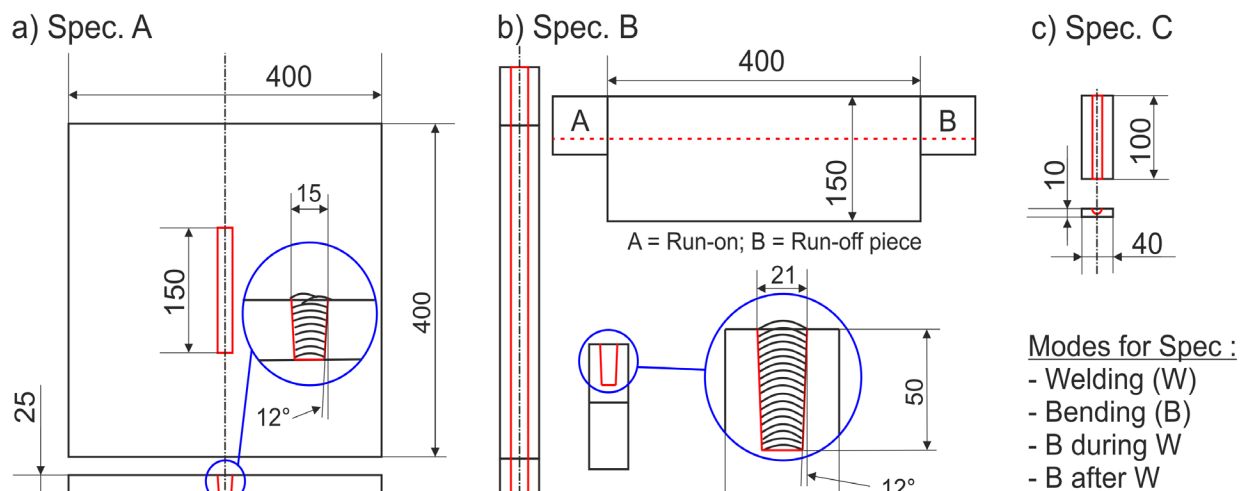


Fig. 2: Specimen types: (a) Spec A: Slit specimen, (b) Spec B: U-shape notch, (c) Spec C: Small-scale specimen

- Modes for Spec. C:
- Welding (W)
 - Bending (B)
 - B during W
 - B after W

The chemical composition of the base material (BM) and the deposited filler/weld metal (WM) are shown in Table 1 [5]. Additionally, it contains the mechanical properties. The corresponding welding parameters are shown in Table 2.

Table 1: Chemical composition of BM, deposited WM and mechanical properties [5]

	Content [wt.-%], Rest Fe									R _{p0.2} [MPa]	R _m [MPa]	A ₅ [%]
	C	Si	Mn	Cr	Cu	Mo	Ni	V	Nb			
BM	0.12	0.08	0.51	2.29	0.11	0.98	0.12	0.30	0.03	607	725	22
WM	0.07	0.08	1.23	2.27	0.04	0.96	0.16	0.23	0.01	415*	600*	18*

* Specifications from welding consumable supplier after PWHT at 705 °C for 4 h

Table 2: Layer sequence and welding parameters of Spec. A to C

Sample	Layer number	Load condition	Weld speed [mm/s]	Current [A]	Voltage [V]	Heat input [kJ/mm]
Spec. A	10	Self-restraint	6.0	600	30	~ 3.0
Spec. B	18	Self-restraint	6.0	650/500	34/31	~ 6.8
Spec. C	1	External load	2.0	210	15	~ 1.5

Spec. A and B were joint by SAW process (wire-Ø 4 mm: Spec. A: Single DC-mode and Spec. B: Tandem process DC+AC) with multi-layer technique and represent an approach for self-restraint weld joint samples in accordance to [5, 6]. A disadvantage for a self-restraint specimen is the necessary thickness. Hence, Spec. C was focused on inducing comparable mechanical stresses. For that reason, the weld heat input was simulated by high-energy TIG (tungsten inert gas) weld arc and an adapted test facility [8]. This facility offers a superimposed mechanical bending of the specimen perpendicular to the weld direction [8]. Four different conditions of Spec. C have been examined: (I) pure bending, (II) pure welding, (III) bending during welding and (IV) bending after welding. Conditions I and II were the reference conditions III and IV were used to simulate similar load conditions as occurred in self-restraint Spec. A and B but with significantly smaller specimen size (see Fig. 2). All specimens were in as-welded condition without further PWHT. The reason is that the initial residual stresses are important for SRC susceptibility. Hence, the as-welded condition must be compared prior to further PWHT.

The local longitudinal residual stresses were determined in each case by X-ray diffractometry (*Stresstech G3*) using the $\sin^2\psi$ -technique [9]. The stresses were measured on the specimen's top surface across the weld (Spec. C only), the HAZ and the base material using a step size of 1 mm, further parameters can be found in [10].

Results and Discussion

Spec. A - Slit specimen. The longitudinal residual stress is shown in Fig. 3 (left). Tensile residual stresses up to 400 MPa were found in the HAZ approximately 3 mm from the fusion line. In transition to the weld metal the stresses tended to decrease but remained tensile. Note, that due to microstructural reasons no reliable stress determination was possible in the weld metal itself. Adjacent to the HAZ large stress gradients were found. With increasing distance to the HAZ the stresses quickly drop into compression around -100 MPa. With larger distance compressive values about -200 MPa were present in the base material. The same compressive stress level was found in transverse direction as indicated in Fig. 3 (right). In the HAZ still a compressive stress level was present. The transition into the weld metal was just characterized by -50 MPa, respectively 0. The stress distribution was not symmetric to the weld centre as the

layers were deposited eccentrically. As a result, high tensile residual stress peaks were present in longitudinal direction in the HAZ. The transverse residual stresses are much lower [5, 11].

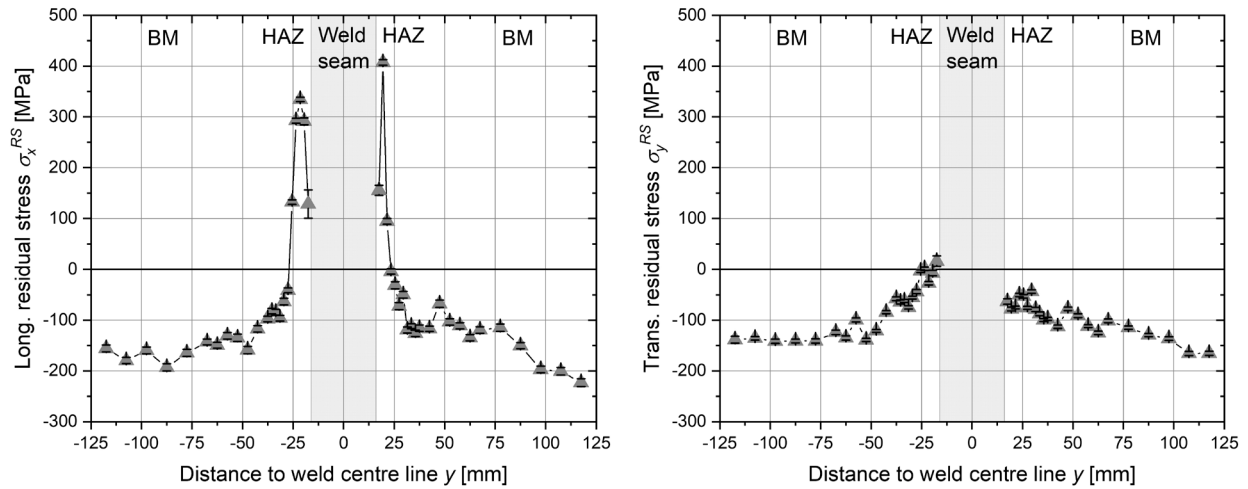


Fig. 3: Longitudinal (left) and transverse residual stresses (right) in Spec. A

Spec. B - U-shape notched specimen. The U-shape notched specimen had only a small width of 42 mm. The longitudinal residual stresses shown in Fig. 4 (left) indicate that the high tensile stresses are located on the edges of the fillets. The HAZ extends here about the whole width of the specimen. The stress level is comparable to the slit specimen with maximum values around 400 MPa. Towards the weld metal the stresses drop into compression. This gradient is larger than observed for the slit specimen. The low restraint acting in transverse direction causes compressive stresses in transverse direction, see Fig. 4 (right). Their level is even lower compared to the slit specimen. The special shape of the U-notched specimen leads to comparable longitudinal residual stresses as found in the heavy slit specimen. However, the transverse residual stresses are neglectable. High tensile residual stress maxima located in the HAZ are characteristic for transformation affected welds. Similar residual stress distributions are known from high-strength steel welds [6, 12, 13].

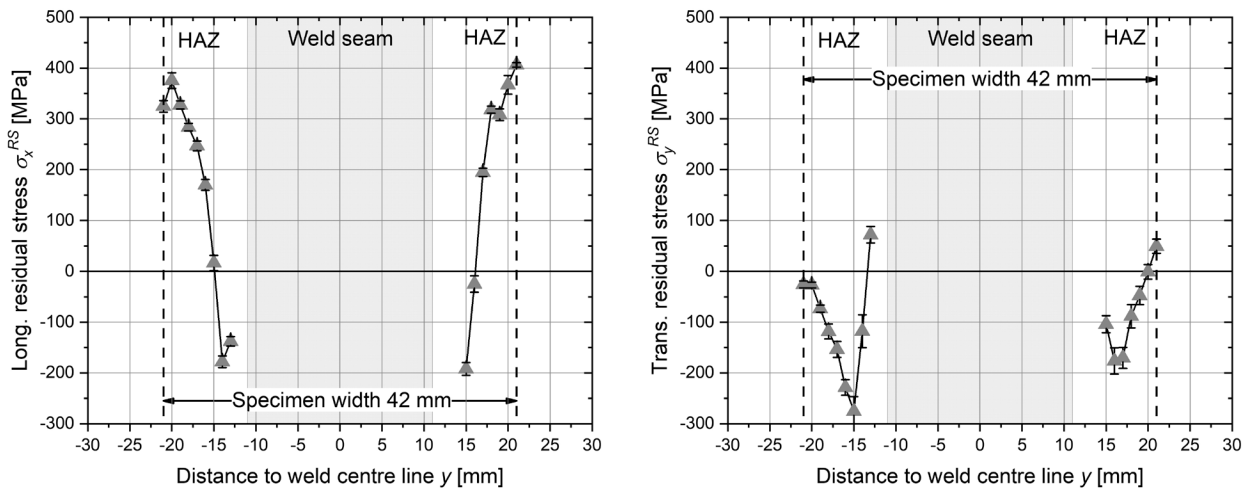


Fig. 4: Longitudinal (left) and transverse residual stresses (right) in Spec. B

Spec. C - Small-scale Specimens. For testing of the small-scale specimens, a mechanical bending was additionally applied longitudinal to the welding direction. Fig. 5 shows the longitudinal residual stresses for the four different states derived from the experiments.

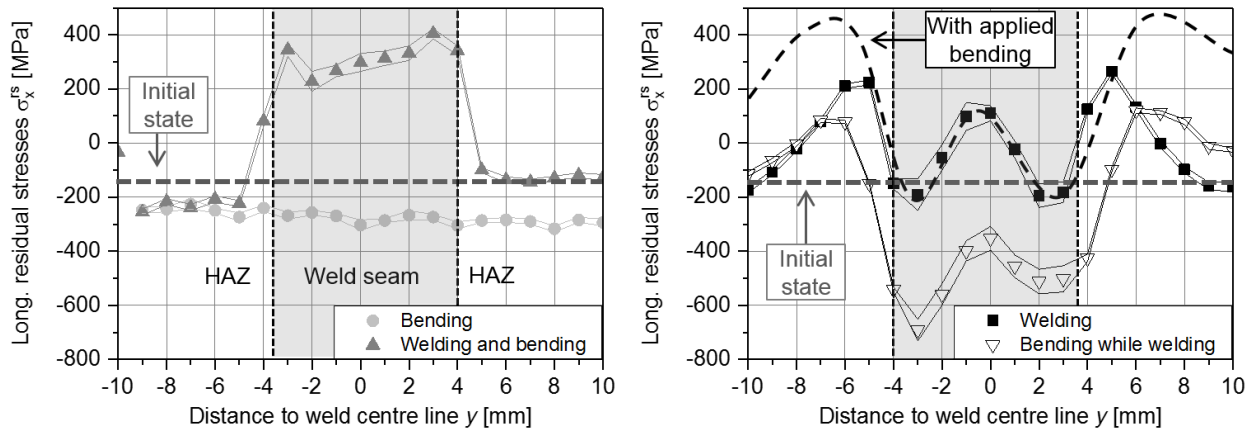


Fig. 5: Spec C - Longitudinal residual stress distributions for the four experimental conditions

While simply bending of the specimen, a plastic deformation of the top side of the specimen is observable. After release of the specimen from the testing machine a spring back occurs, which leads to higher compressive residual stresses (approx. -300 MPa) at the top side compared to the initial state of about -150 MPa.

Solitary welding of the specimen affects longitudinal stress distributions as typical for steel with undergoing phase transformation [12, 13]. The surface of the weld seam shows a stress maximum of 100 MPa at weld center and compressive stresses down to -200 MPa near the fusion line, which is due to the volume expansion of the phase transformation while cooling of the weld. The restraint of the cooler weld vicinity leads therefore to an increase of the residual stresses in the heat effected zone due to shoring effects. Tensile residual stress maxima of over 200 MPa can be observed in the HAZ.

The highest tensile residual stresses (400 MPa) can be observed in the weld seam, if the specimen is welded and subsequently bending is applied while cooling of the specimen. The transformation stresses are completely suppressed due to the superimposing bending stresses while cooling. Therefore, no shoring effects towards the weld vicinity were observed and the residual stresses in the HAZ are at the amount of the initial state.

In the last case the superposition of stresses at the weld top side due to additional bending at high temperatures while welding causes a plastic deformation with almost no resistance of the whole weld zone. After welding, subsequent cooling of the bended specimen leads to major evolution of welding residual stresses. At room temperature, the specimen is released from the testing machine as are the superimposed bending stresses, which affects a spring back of the specimen and a translation of the weld topside tensile residual stresses to compressive stress values from -700 to -350 MPa. Compared to the weld seam stresses without additional bending, the resulting residual stresses are approx. 400 MPa lower in the weld seam. The weld vicinity shows only stress differences from -100 to 100 MPa. However, if it is presumed that the translation of the stresses due to the spring back are constant over the whole specimen top side, the result would be high tensile residual stresses of 400 to 500 MPa in the HAZ due to the shoring effects, restraint shrinkage and bending stresses. This shows an important aspect for component relevant testing using small-scale specimen, especially in terms of weld cracking investigation.

Summary

The presence of high tensile residual stresses is a prerequisite for SRC during PWHT of creep-resistant CrMoV steels. The residual stresses resulting from the welding process are strongly determined by the boundary conditions resulting from the production of large welding components. Testing such scenarios on the laboratory scale is elaborate. In the present study, three different welding tests (Spec. A to C) were evaluated using XRD regarding the residual stresses that occur. The tests differ in size and complexity. In the heavy slit specimen (Spec. A) high tensile residual stresses were found in the HAZ in longitudinal direction. A special U-shaped notch specimen (Spec. B) also provided comparable residual stress levels in the HAZ. On the other hand, the transverse residual stresses in both tests were negligible. Small-scale bead-on-plate welds (Spec. C) gave similar residual stress distributions, but with lower peak values in the HAZ. Additional mechanical bending raised the stresses over the entire seam area to a level comparable to the other two tests. Thus, even this small sample can be used to a limited extent to simulate corresponding residual stresses with justifiable effort. Further modifications are planned.

References

- [1] L. Antalffy, Metallurgical, design & fabrication aspects of modern hydroprocessing reactors, *Weld. Res. Counc. Bull.* 524 (2009) 77-115.
- [2] K. Park et al., Post-weld heat treatment cracking susceptibility of T23 weld metals for fossil fuel applications, *Mater. Des.* 34 (2012) 699-706. <https://doi.org/10.1016/j.matdes.2011.05.029>
- [3] K. Tamaki, J. Suzuki, H. Kawakami, Metallurgical factors affecting reheat cracking in HAZ of Cr-Mo steels. *Proceedings of the Finnish-German-Japanese Joint International Seminar on Mechanical Approaches to New Joining Process* (2004), 155-168.
- [4] P. Nevasmaa, J. Salonen, Reheat Cracking Susceptibility and Toughness of 2% CrMoWVNb P23 Steel Welds, *Weld. World.* 52(3) (2008) 68-78. <https://doi.org/10.1007/BF03266633>
- [5] T. Lausch, *Zum Einfluss der Wärmeführung auf die Rissbildung beim Spannungsarmglühen dickwandiger Bauteile aus 13CrMoV9-10*, BAM Dissertationsreihe 134, Berlin, 2015.
- [6] D. Schroepfer, A. Kromm, T. Kannengiesser, Load analyses of welded high-strength steel structures using image correlation and diffraction techniques, *Weld. World.* 62(3) (2018) 459–469. <https://doi.org/10.1007/s40194-018-0566-x>
- [7] DIN EN 10028-2, Flat products made of steels for pressure purposes - Part 2: Non-alloy and alloy steels with specified elevated temperature properties, German version (2017).
- [8] T. Kannengiesser, T. Boellinghaus, Hot cracking tests-an overview of present technologies and applications, *Weld. World.* 58(3) (2014) 397-421. <https://doi.org/10.1007/s40194-014-0126-y>
- [9] E. Macherauch, P. Müller, Das $\sin^2\psi$ - Verfahren der röntgenografischen Spannungsmessung, *Zeitschrift für angewandte Physik* 13 (1961) 305-312.
- [10] M. Rhode, A. Kromm, T. Kannengiesser, Residual stresses in multi-layer component welds, in: T. DebRoy et al. (Eds.), *Trends in Welding Research: Proceedings of the 9th International Conference*, ASM International, Materials Park (Ohio), 2013, pp. 48-54. <https://doi.org/10.1016/j.jmatprotec.2013.01.008>
- [11] T. Lausch, T. Kannengiesser, M. Schmitz-Niederrau, Multi-axial load analysis of thick-walled component welds made of 13CrMoV9-10, *J. Mater. Process. Tech.* 213(7) (2013) 1234-1240. <https://doi.org/10.1016/j.jmatprotec.2013.01.008>
- [12] T. Nitschke-Pagel, H. Wohlfahrt, Residual stresses in welded joints - Sources and consequences, *ECRS 6: Proceedings of the 6th European Conference on Residual Stresses*, 2002, pp. 215-224.
- [13] M. Farajian, R.C. Wimpory, T. Nitschke-Pagel, Relaxation and Stability of Welding Residual Stresses in High Strength Steel under Mechanical Loading, *Steel. Res. Int.* 81(12) (2010) 1137-1143. <https://doi.org/10.1002/srin.201000194>